Accessing Structure and Dynamics of Mobile Phase in Organic Solids by Real-Time T-1C Filter PISEMA NMR Spectroscopy

ARTICLE *in* THE JOURNAL OF PHYSICAL CHEMISTRY A · DECEMBER 2011

Impact Factor: 2.69 · DOI: 10.1021/jp2078902 · Source: PubMed

6 AUTHORS, INCLUDING:

Rongchun Zhang
University of Michigan
27 PUBLICATIONS **122** CITATIONS
SEE PROFILE

Pingchuan Sun
Nankai University
119 PUBLICATIONS **1,539** CITATIONS
SEE PROFILE

THE JOURNAL OF PHYSICAL CHEMISTRY A

ARTICLE

pubs.acs.org/JPCA

Accessing Structure and Dynamics of Mobile Phase in Organic Solids by Real-Time T_{1C} Filter PISEMA NMR Spectroscopy

Rongchun Zhang,[‡] Yuzhu Chen,[†] Tiehong Chen,[†] Pingchuan Sun,*[,†] Baohui Li,*[,‡] and Datong Ding[‡]

[†]Key Laboratory of Functional Polymer Materials, Ministry of Education, College of Chemistry, Nankai University, Tianjin 300071, People's Republic of China

[‡]School of Physics, Nankai University, Tianjin 300071, People's Republic of China

Supporting Information

ABSTRACT: The structure and dynamic behavior of mobile components play a significant role in determining properties of solid materials. Herein, we propose a novel real-time spectrum-editing method to extract signals of mobile components in organic solids on the basis of the polarization inversion spin exchange at magic angle (PISEMA) pulse sequence and the difference in ^{13}C T_1 values of rigid and mobile components. From the dipolar splitting spectrum sliced along the heteronuclear dipolar coupling dimension of the 2D spectrum, the structural and dynamic information can be obtained, such as the distances between atoms, the dipolar coupling strength, the order parameter of the polymer backbone chain, and so on. Furthermore, our proposed method can be used to achieve the separation of overlapped NMR signals of mobile and rigid phases in the PISEMA experiment. The high efficacy of this 2D NMR method is demonstrated on organic solids, including crystalline L-alanine, semicrystalline polyamide-6, and the natural abundant silk fibroin.

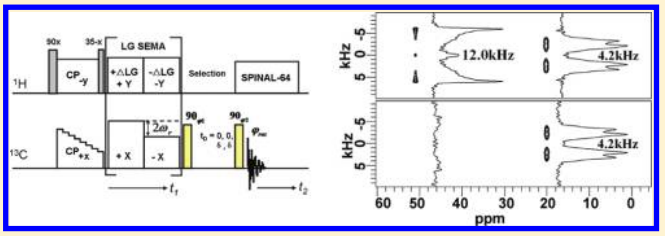

1. INTRODUCTION

Molecular dynamics is ubiquitous and exerts important effects on mechanical properties and electronic conductivity of a polymer,[1,2] activity of proteins,[3] stability of pharmaceuticals,[4] and transport properties in membranes,[5] as well as the behavior of amorphous materials near the glass transition.[6] In particular, the mobile component plays a crucial role in determining the physical and chemical properties, as well as the functions of polymers and proteins. For example, the mobile phase could, to a great extent, change the topological constraints imposed by the crystallites of polymers, which could make a high-strength material become extremely tough.[7,8] Besides, in the pharmaceutical industry, the stability of amorphous pharmaceuticals against crystallization is quite important in enhancing the bioavailability.[9] Furthermore, the mobile components exert vital influence on the conductivity of a solid polymer electrolyte.[10,11] Therefore, developing new techniques to get detailed information of the structure and dynamics of the mobile phase in organic solids is rather pressing.

Since its emergence decades ago, solid-state NMR has identified itself as a powerful probe of molecular structures and dynamics in solids.[12−17] Polarization inversion spin exchange at magic angle (PISEMA) is a novel two-dimensional (2D) separated-local-field (SLF) experiment that correlates the orientation-dependent, anisotropic heteronuclear dipolar coupling with the chemical shift of low γ nuclei.[18] In the recent decade, PISEMA was extensively used to study the structure and dynamics of synthetic polymers,[3] liquid crystal,[19,20] especially the function and secondary structure of proteins.[21] A PISEMA spectrum may contain wheel-like patterns of peaks, which has been shown to provide the topology of the helix in an aligned helical membrane protein, the amplitude and geometry of the molecular motions in biomacromolecules and solid polymers.[22,23] In addition, it was found to be quite useful in assigning overlapped signals in 1D spectrum.[24] However, when it comes to organic solids with complex molecular mobility and overlapped signals for individual chemical groups, there is still no efficient method to directly obtain the structural and dynamical information of the mobile phase with a high resolution and sensitivity.

Recently, a novel NMR method[25] was proposed by Mowery et al. to successfully obtain the information of intermediate components through incorporating "inverse ^{13}C T_1 filter" into cross-polarization (CP) and 2D wide-line separation (WISE)[26] pulse sequences. As the final spectrum was achieved by subtraction of two spectra which were acquired respectively with different delay time in the pulse of inverse ^{13}C T_1 filter, the results were very sensitive to the field shift as well as radiofrequency power instability. Likewise, by effectively combining Torchia's T_1 filter pulses[27] and PISEMA sequences,[28,29] the rigid component can be well resolved in PISEMA-type experiments with a good resolution and sensitivity.[28,29] However, to make it applicable for the investigation of mobile phase, the initial cross-polarization

Received: August 17, 2011
Revised: December 5, 2011
Published: December 20, 2011

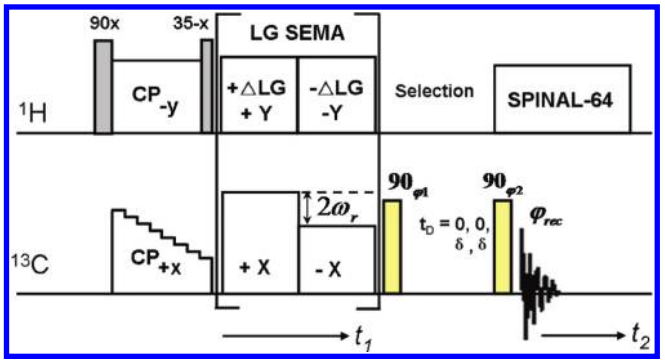

Figure 1. Schematic representation of the 2D RT_PISEMA pulse sequence with flip-back and read-out pulses to separate the signals of rigid and mobile components. CP: cross-polarization. SPINAL-64: dipolar decoupling pulses. φ_1 = 270, 90, 270, 90; φ_2 = 90; t_D = 0, 0, δ, δ; φ_{rec} = 0, 180, 180, 0. The delay time δ is usually set as 3−5 times T_{1C} of the mobile signals if the T_{1C} for the rigid components is much greater than that for mobile components.

process was replaced with a train of saturation pulses to suppress ^{13}C magnetization of the crystalline phase,[28] referred to as direct polarization SEMA with presaturation (DP_SEMA). As a result, the ^{13}C magnetization of the mobile components was greatly reduced due to the lack of $^{1}H \rightarrow {}^{13}C$ cross-polarization before the heteronuclear recoupling period, and hence the advantage of high ^{13}C signal sensitivity in PISEMA experiments is totally lost in that experiment.

In this work, we propose a novel real-time T_{1C} filter PISEMA (referred to as RT_PISEMA) experiment on the basis of the inverse ^{13}C T_1 filter and a special four-step phase cycling. This experiment can efficiently select the mobile signals and keeps the advantages of the PISEMA-type experiments. Moreover, the overlapped signals between rigid and mobile components can be well separated by using our proposed method. The capability of this new real-time spectrum-editing 2D NMR method is well demonstrated on organic solids including crystalline L-alanine, semicrystalline polyamide-6 and the natural abundant silk fibroin.

2. PULSE SEQUENCE

Our proposed pulse sequence of 2D RT_PISEMA experiment is shown in Figure 1. It contains the basic PISEMA sequence followed by inverse ^{13}C T_{1C} filter composed of a pair of 90° pulses between which there is a period of delay time, t_D. By analyzing the signal compositions after each step of the phase cycling, the basic principle of our approach to efficiently select the mobile signals in PISEMA experiment can be easily understood. When t_D = 0, except the two flip-back and read-out 90° pulses, this sequence is just the same as a standard PISEMA experiment,[30] and therefore both rigid and mobile signals can be obtained at the meantime without any loss. The flip-back and read-out 90° pulses in succession can minimize the baseline distortion to a great extent.[28]

At the first step of phase cycling, t_D = 0, φ_1 = 270, φ_2 = 90, and the signal before the receiver can be obtained as

$$S_1 = S_0 + S_{mobile} + S_{rigid}$$

where S_0 refers to the artificial signals induced by the background, baseline distortion, and so on, and S_{mobile} and S_{rigid} correspond to the mobile and rigid signals, respectively.

At the second step of phase cycling, t_D = 0, φ_1 = 90, φ_2 = 90, and the signal before the receiver is

$$S_2 = S_0 - (S_{mobile} + S_{rigid})$$

Besides, generally speaking, in most organic solids the relaxation time of rigid component T_{1C}^{rigid} is considerably larger than that of mobile component T_{1C}^{mobile}, sometimes even by several orders of magnitude. Therefore, when t_D is set as δ (generally slightly larger than $3*T_{1C}^{mobile}$), the magnetization of mobile signals can be fully suppressed by ^{13}C spin−lattice relaxation, while the rigid signals are almost completely retained.

So, at the third step of phase cycling, $t_D = \delta$, φ_1 = 270, φ_2 = 90, and the signal before the receiver is

$$S_3 = S_0 + S_{rigid}$$

At the fourth step of phase cycling, $t_D = \delta$, φ_1 = 90, φ_2 = 90, and the signal before the receiver is

$$S_4 = S_0 - S_{rigid}$$

For each above step, the phase of receiver is 0, 180, 180, and 0, respectively; therefore, the final detected signal is

$$S_{final} = (S_1 - S_2) - (S_3 - S_4) = 2S_{mobile}$$

Then a 2D PISEMA spectrum with the pure mobile phase signals is obtained. Therefore, it is convenient to directly get the real-time FID signals of the pure mobile components at the acquisition period, which can be well used to optimize the experimental parameters so as to improve the signal-to-noise ratio of spectrum and to save experimental time. Compared to other spectrum-editing methods, the real-time spectrum-editing NMR technique exhibits unique superiority in obtaining a real-time difference spectrum and removing the influence of the instability of radio frequency power and magnetic field. It offers an exciting possibility to obtain highly resolved site-specific dipolar profiles with high sensitivity to clearly elucidate the microstructure and dynamics of the mobile component in organic solids, including small molecules, polymers, and proteins. However, as shown above, only two of four transients contain the mobile signals in the four-step phase cycling; therefore, the sensitivity of our method is only half of that of PISEMA with the same experimental parameters, but it is still higher than that of DP_SMEA,[28] as shown in Figure 2. Furthermore, it should be emphasized that the delay time δ at the third and fourth step of phase cycling is the most important parameter for acquiring a good 2D RT_PISEMA spectrum with pure mobile signals. In most cases, the T_{1C}^{rigid} is much larger than T_{1C}^{mobile}; therefore, a delay time of $3T_{1C}^{mobile}$ can well relax the signals of mobile components while simultaneously completely retaining rigid signals. Nevertheless, when the difference between T_{1C}^{rigid} and T_{1C}^{mobile} is not large enough, the delay time δ has to be carefully considered for obtaining only mobile signals. Generally, $\delta = T_{1C}^{mobile}$ is long enough. If δ is too small, the mobile signals will not completely relax, which directly resulted in a poor sensitivity for the mobile components in the final spectrum. But if it is too large, there may be a little loss of rigid signals, resulting in residue signals of rigid components in the RT_PISEMA spectrum. Therefore, in most cases, it is well suggested to acquire a real-time T_{1C} filter ^{13}C CP/MAS spectrum in order to make sure that a higher selectivity is obtained for mobile signals and the rigid signals are completely subtracted in the final difference spectrum. By the way, it should be mentioned that using only third and

dx.doi.org/10.1021/jp2078902 |J. Phys. Chem. A 2012, 116, 979–984

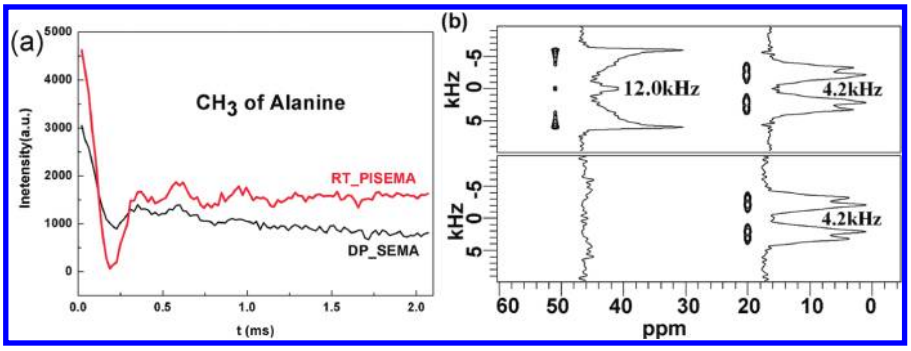

Figure 2. (a) Dipolar coupling evolution time (t_1) dependence of ^{13}C signal intensity of L-alanine CH_3 units obtained by RT_PISEMA and DP_SEMA[28] pulse sequences. The optimized experimental parameters for the two experiments are exactly the same. (b) 2D NMR spectra for L-alanine by PISEMA (top) and RT_PISEMA (bottom). $^{13}C-^{1}H$ dipolar splitting spectrum for CH and CH_3 groups, and the splitting values are also shown in the figures. In the experiments, na = 8.

fourth step phase cycling with $t_D = \delta$ is enough for rigid signal selection.

3. EXPERIMENTAL SECTION

Samples. Three samples were used to test the proposed pulse sequence. L-Alanine was purchased from Aldrich Chemical Co., Inc. Polyamide-6 and Cocoons of *B. mori* silkworm silk were commercially available. All the samples are directly used for the experiments without further treatment.

Nuclear Magnetic Resonance (NMR) Experiments. Solid-state NMR experiments were performed on a Varian Infinityplus-400 spectrometer at a frequency of 100.5 MHz for ^{13}C and 399.7 MHz for ^{1}H. All experiments were carried at room temperature (25 °C). A conventional 4 mm double-resonance HX CP/MAS NMR probe was used, and samples were placed in a 4 mm zirconia PENCIL rotor with 52 μL sample volume. The magic angle spinning (MAS) was automatically controlled at 12 kHz within ±1 Hz with a MAS speed controller for all experiments. The ^{13}C chemical shifts were referenced to external HMB (hexamethylbenzene, δ_{iso} = 17.3 ppm for CH_3 group). Initial ^{13}C transverse magnetization was created by ramped $^{1}H-^{13}C$ CP, and the contact time was set as 0.6 ms. The ^{13}C field strength was amplitude modulated to fulfill Hartmann−Hahn matching condition[31] at +1 and −1 spinning sideband so that the difference in amplitude between the two RF fields was equal to $2\omega_r$, where ω_r is the spinning speed of the rotor. The Lee−Goldburg (LG) pulse sequence was adopted for proton homonuclear decoupling during the SEMA period, and the radio frequency power was relatively high at 79 kHz, corresponding to a 3.169 μs 90° pulse. Heteronuclear decoupling during the acquisition period was achieved by SPINAL-64 irradiation. For all the RT_PISEMA experiments, the delay time δ is carefully set to make sure that the mobile signals are fully relaxed, while the rigid signal is almost completely sustained. The number of acquisitions per increment (na) in the dipolar coupling dimension varied for different experiments. Exact values are shown in the figure captions.

4. RESULTS AND DISCUSSION

The high selectivity of mobile signals for RT_PISEMA pulse sequence is well demonstrated on several typical samples in this section. Figure 2a shows a comparison of the $^{13}C-^{1}H$ dipolar oscillation (FID in the t_1 dimension, referred to as FID(t_1)) of the mobile CH_3 group of L-alanine obtained from RT_PISEMA and DP_SEMA[28] under the same optimized experimental conditions. Obviously, the FID(t_1) of RT_PISEMA has a larger amplitude at the initial t_1 value, which means a better signal sensitivity. Moreover, it becomes flat at longer spin exchange time ($t_1 \sim 2$ ms), so there will be a weak zero frequency peak after Fourier transformations in F1 dimension. In contrast, the FID of DP_SEMA[28] indicates an inferior signal sensitivity and a strong zero frequency peak due to the obvious decay of FID(t_1) at long t_1 values. It is not difficult to understand the difference, as the polarization inversion along the direction of magic angle in the RT_PISEMA can greatly enhance the signals,[32] whereas in DP_SEMA, the polarization inversion is intentionally kept away to avoid the $^{1}H \rightarrow {}^{13}C$ spin exchange of the mobile signals. What's worse, in DP_SEMA, spin-locking of the ^{13}C magnetization of the mobile components will pass on to ^{1}H nuclei during the SEMA recoupling period, which also reduces the ^{13}C magnetization greatly.[28] Figure 2b shows the 2D PISEMA and RT_PISEMA spectra of L-alanine, where we can clearly see that the latter can directly achieve a pure $^{13}C-^{1}H$ dipolar spectrum of the mobile group ($-CH_3$), which is exactly the same as that obtained in the former, while the rigid signal ($-CH$) is almost completely suppressed. Certainly, the rigid signals ($-CH$) can also be directly obtained with RT_PISEMA by changing the delay time t_D to a fixed value in T_{1C} filter to relax mobile signals with simultaneously proper phase cycling (data not shown here).

In general, the molecular motions are closely related with the heteronuclear coupling strength which is well represented by the dipolar splitting along the heteronuclear dipolar coupling dimension of PISEMA-type spectrum. As a 2D spectrum containing only the signals of pure mobile components, RT_PISEMA provides wealth of information about the structure and dynamics. For example, from a RT_PISEMA spectrum, we can discriminate the various chemical groups different in mobility, and obtain the dipolar coupling strength, the direction of chemical bonds as well as the distances between atoms. From the dipolar splitting spectra of the $-CH_3$ and $-CH$ groups in Figure 2b, the $^{13}C-^{1}H$ dipolar coupling strength, $^{13}C-^{1}H$ distance and their direction relative to the magnetic field for individual group may easily be determined.[21] Besides, the bond order parameter can be obtained from the ratio of motion reduced dipolar coupling and the static rigid-limit dipolar coupling constants, $S_{bond} = D_{res}/D_{static}$.[3] Then the order parameter of the polymer backbone could be achieved as $S_{backbone} = k \times D_{res}/D_{static} = 0.6 \times r^2/N$, where r is

dx.doi.org/10.1021/jp2078902 |J. Phys. Chem. A 2012, 116, 979–984

the end-to-end vector of the chain segment separating the constraints, and N is the number of statistical segments between constraints.[33] Moreover, the backbone order parameter can be correlated with the segmental autocorrelation function,[33,34] which may be further used to study the variation of polymer chain motion with time.

Most of the $^{13}C-^{1}H$ PISEMA NMR spectra of semicrystalline polymers contain overlapped signals arising from the crystalline and amorphous regions, especially for those with different crystal forms, such as semicrystalline polyamide-6, a widely used industrial material[35] containing α- and γ-crystalline phases. Polyamide-6 has attracted great attention during the past decades for its special mechanical strength and toughness.[36−38] Nevertheless, to extract detailed structural and dynamic information from PISEMA spectrum with seriously overlap ^{13}C signals in this polymer is still a great challenge.[39] Polyamide-6 contains α- and γ-crystals in rigid crystalline domain and mobile amorphous domain, and the ^{13}C T_1 values of the chemical groups in rigid and mobile domains are obviously different by more than 1 order of magnitude due to their large difference in molecular mobility. So, herein, RT_PISEMA once again presents its superiority in efficient selection of the mobile signals of amorphous domain in this semicrystalline material, as shown in Figure 3. In the PISEMA spectrum, the projection of methylene units (20−50 ppm) along ^{13}C chemical shift dimension indicates a serious overlap of crystalline (α- andγ-form) and amorphous signals (see Figure S1 and Table S1 in the Supporting Information for the chemical shift assignment of each peak), while for the RT_PISEMA experiment, the projection only contains the broad amorphous signals due to the rapid ^{13}C T_1 relaxation of the mobile signals during ^{13}C T_1 filter and the real-time spectrum difference. We also show the dipolar splitting spectra at about 30 ppm and 37 ppm for the PISEMA and RT_PISEMA spectrum, respectively, in Figure 3c,d, which clearly indicate the efficient selection of the mobile signals judged from the dipolar splitting values. This example clearly illustrates how the real-time T_{1C} filter method can be effectively used to reveal the structure and dynamic information in a complex system with seriously overlapped ^{13}C signals of both rigid and mobile components.

As an advanced NMR technique, PISEMA has also proved its power and efficacy in the research of protein's structure and dynamics.[21,22] As another demonstration, we also show the feasibility of RT_PISEMA in elucidating the structure and dynamics of silk fibroin, a natural abundant protein which has attracted tremendous attention in the past decades as one of promising resources of biomedical materials due to its remarkable mechanical properties and excellent biocompatibility, good oxygen and water vapor permeability, biodegradability, and minimal inflammatory reaction.[40−42] However, few NMR work was reported concerning the local dynamics of the different chemical groups in silk fibroin.

The *Bombyx mori* silk fibroin contains a repetitive sequence (Gly-Ala-Gly-Ala-Gly-Ser)n as well as small amounts of tyrosine (Tyr) and valine (Val).[43] As shown in Figure 4a, the 2D $^{13}C-^{1}H$ PISEMA spectrum exhibits complicated signals for different chemical groups of amino acids (see Figure S2 and Table S2 for the chemical shift assignment of each peak). However, in RT_PISEMA spectrum, only mobile signals are retained, and according to the spectrum in Figure 4b, it is obvious that Ala $-CH_3$ (ca. 20 ppm) and Ser $-CH_2OH$ (ca. 63 ppm) groups exhibit higher mobility compared to other groups, which may play an important role in stabilizing the solid structure of silk proteins.[44] Due to the extremely low content of the mobile

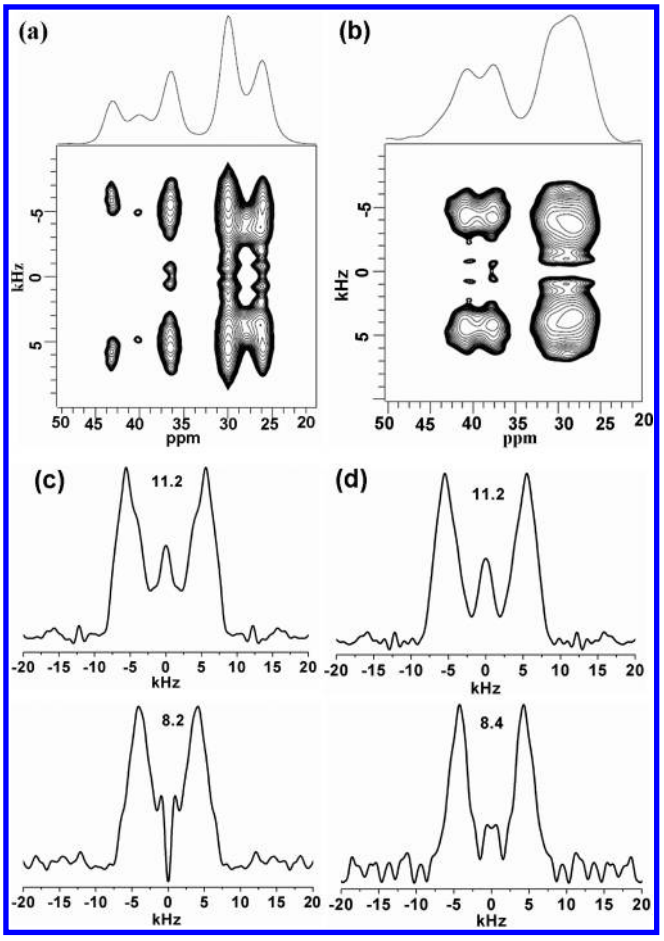

Figure 3. 2D NMR spectra for polyamide-6 by (a) PISEMA, na = 256 and (b) RT_PISEMA, na = 200. The $^{13}C-^{1}H$ dipolar splitting spectra at about (c) 30 and (d) 37 ppm are sliced from the PISEMA spectrum (top) and RT_PISEMA spectrum (bottom). Projections of the spectra in the ^{13}C chemical shift dimension are shown on the top of the 2D spectra. The delay time δ in T_1 filter of the RT_PISEMA experiment is 2 s.

serine, its signal is so weak that it is comparable to the noise. And as shown in the inset of Figure 4b, the $^{13}C-^{1}H$ dipolar splitting value for the highest peaks is 8.5 kHz, which is a typical dipolar splitting value for mobile components as detected in polyamide-6. In contrast, the other outer larger splitting peak can be reasonably attributed to the noise. RT_PISEMA can further reveal the quantitative information of the dynamics through the spitting of the dipolar spectra sliced from the 2D spectrum, which is quite convenient for determining the heteronuclear coupling strength as well as distances between atoms in the mobile components. Furthermore, to a degree, it can help us understand the mechanism of conformational transition of silk fibroin from a random coil to a β-sheet under different conditions.[45] The same as silk fibroin, spider silk also possess superior mechanical properties,[8,46] and it is expected that RT_PISEMA may facilitate our recognition of the mechanism for its excellent strength and toughness at molecular level. Because the PISEMA-type spectra contain information about both structure and dynamics, further studies may help us to understand and elucidate the origin of the excellent mechanical properties of silk fibroin. It should be noted that our proposed method may suffer from certain limitations in creating initial ^{13}C signal intensity for the extremely mobile components in the sample due to their much smaller dipolar coupling. In that case,

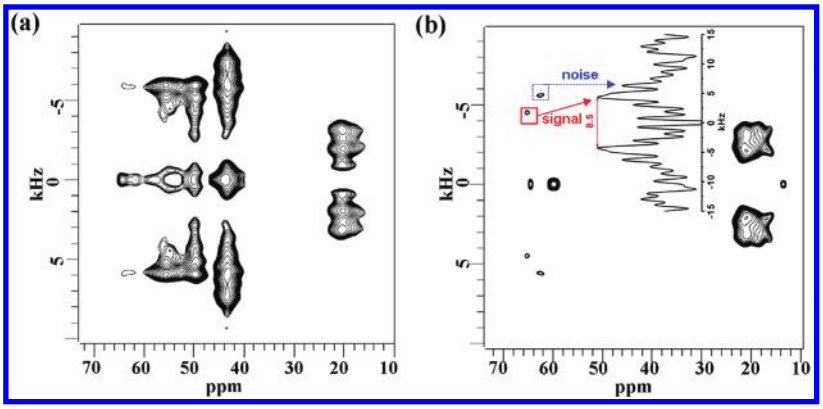

Figure 4. 2D NMR spectra for natural silk fibroin by (a) PISEMA, na = 400 and (b) RT_PISEMA, na = 1500. In the latter figure, the $^{13}C-^{1}H$ dipolar splitting spectrum at about 63 ppm is also shown. The $^{13}C-^{1}H$ dipolar splitting value for the highest peak is 8.5 kHz, which is caused by the mobile serine, while the other outer splitting peak is actually caused by the noise. The delay time δ, in T_1 filter of the RT_PISEMA experiment, is set as 0.8s.

DP_SEMA could be a good choice.[28,47] But, in most cases, cross-polarization creates a higher initial signal intensity than direct polarization in organic solids.

5. CONCLUSION

In summary, a novel real-time T_{1C} filter PISEMA pulse sequence (RT_PISEMA) is proposed to efficiently select the mobile signals in organic solids, even when the signals of both mobile and rigid components are completely overlapped. Our proposed real-time spectrum-editing method overcomes the disadvantage of the general spectrum-editing method in several aspects, such as the sensitivity to the instability of radiofrequency power and magnetic field. The high efficacy of the proposed method is well demonstrated on several organic solids, including crystalline L-alanine, semicrystalline polyamide-6, and the natural abundant silk fibroin. Although we have only given limited demonstration of the application of RT_PISEMA experiment, we believe that this technique will be also highly valuable in the structural and dynamic studies of biological molecules such as membrane-associated peptides and proteins or the liquid crystals.

■ ASSOCIATED CONTENT

Supporting Information. The schematic diagram for the molecular structures and the chemical shift assignment of peaks for polyamide-6 and silk fibroin are available. This material is available free of charge via the Internet at http://pubs.acs.org.

■ AUTHOR INFORMATION

Corresponding Author

*E-mail: spclbh@nankai.edu.cn; baohui@nankai.edu.cn.

■ ACKNOWLEDGMENT

This work was supported by the National Science Fund for Distinguished Young Scholars (No. 20825416), and the National Natural Science Foundation of China (NSFC) through the General Programs (No. 20774054).

■ REFERENCES

(1) Connor, T.; Read, B.; Williams, G. *J. Appl. Chem.* **1964**, *14*, 74.
(2) Hu, W. G.; Schmidt-Rohr, K. *Polymer* **2000**, *41*, 2979.
(3) Palmer, A. G.; Williams, J.; McDermott, A. *J. Phys. Chem.* **1996**, *100*, 13293.
(4) Andronis, V.; Zografi, G. *Pharm. Res.* **1998**, *15*, 835.
(5) Zhu, F.; Tajkhorshid, E.; Schulten, K. *Biophys. J.* **2002**, *83*, 154.
(6) McKenna, G. B. *Comput. Mater. Sci.* **1995**, *4*, 349.
(7) Loo, L. S.; Cohen, R. E.; Gleason, K. K. *Science* **2000**, *288*, 116.
(8) Nova, A.; Keten, S.; Pugno, N. M.; Redaelli, A.; Buehler, M. J. *Nano Lett.* **2010**, *10*, 2626.
(9) Swallen, S. F.; Kearns, K. L.; Mapes, M. K.; Kim, Y. S.; McMahon, R. J.; Ediger, M. D.; Wu, T.; Yu, L.; Satija, S. *Science* **2007**, *315*, 353.
(10) Massi, M.; Albonetti, C.; Facchini, M.; Cavallini, M.; Biscarini, F. *Adv. Mater.* **2006**, *18*, 2739.
(11) Rhodes, C. P.; Frech, R. *Macromolecules* **2001**, *34*, 2660.
(12) Nagapudi, K.; Leisen, J.; Beckham, H. W.; Gibson, H. W. *Macromolecules* **1999**, *32*, 3025.
(13) Schmidt-Rohr, K.; Spiess, H. W. *Multidimensional Solid-State NMR and Polymers*; Academic Press: London, 1994.
(14) Kim, I.; Han, O. H.; Chae, S. A.; Paik, Y.; Kwon, S.-H.; Lee, K.-S.; Sung, Y.-E.; Kim, H. *Angew. Chem., Int. Ed.* **2011**, *123*, 2318.
(15) Hu, J.; Asbury, T.; Achuthan, S.; Li, C.; Bertram, R.; Quine, J. R.; Fu, R.; Cross, T. A. *Biophys. J.* **2007**, *92*, 4335.
(16) Han, O. H.; Kim, C.-S.; Hong, S. B. *Angew. Chem., Int. Ed.* **2002**, *41*, 469.
(17) Qian, C.; Fu, R.; Gor'kov, P.; Brey, W. W.; Cross, T. A.; Gan, Z. *J. Magn. Reson.* **2009**, *196*, 96.
(18) Wu, C. H.; Ramamoorthy, A.; Opella, S. J. *J. Magn. Reson., Ser. A* **1994**, *109*, 270.
(19) Dvinskikh, S. V.; Yamamoto, K.; Scanu, D.; Deschenaux, R.; Ramamoorthy, A. *J. Phys. Chem. B* **2008**, *112*, 12347.
(20) Ramamoorthy, A. *Thermotropic Liquid Crystals*; Springer: Netherlands, 2007.
(21) Ramamoorthy, A.; Wei, Y.; Lee, D.-K. *Annu. Rep. NMR Spectrosc.* **2004**, *52*, 4103.
(22) Denny, J. K.; Wang, J.; Cross, T. A.; Quine, J. R. *J. Magn. Reson.* **2001**, *152*, 217.
(23) Marassi, F. M.; Opella, S. J. *J. Magn. Reson.* **2000**, *144*, 150.
(24) Narasimhaswamy, T.; Lee, D.-K.; Yamamoto, K.; Somanathan, N.; Ramamoorthy, A. *J. Am. Chem. Soc.* **2005**, *127*, 6958.
(25) Mowery, D. M.; Harris, D. J.; Schmidt-Rohr, K. *Macromolecules* **2006**, *39*, 2856.
(26) Schmidt-Rohr, K.; Clauss, J.; Spiess, H. W. *Macromolecules* **1992**, *25*, 3273.
(27) Torchia, D. A. *J. Magn. Reson.* **1978**, *30*, 613.
(28) Brus, J.; Urbanova, M. *J. Phys. Chem. A* **2005**, *109*, 5050.
(29) Brus, J.; Urbanova, M.; Kelnar, I.; Kotek, J. *Macromolecules* **2006**, *39*, 5400.
(30) Dvinskikh, S. V.; Zimmermann, H.; Maliniak, A.; Sandstrom, D. *J. Magn. Reson.* **2003**, *164*, 165.

(31) Hartmann, S. R.; Hahn, E. L. *Phys. Rev.* **1962**, *128*, 2042.
(32) Hong, M.; Yao, X.; Jakes, K.; Huster, D. *J. Phys. Chem. B* **2002**, *106*, 7355.
(33) Saalwachter, K. *Prog. Nucl. Magn. Reson. Spectrosc.* **2007**, *51*, 1.
(34) Vaca, C.; aacute; vez, F.; Saalw; auml; chter, K. *Phys. Rev. Lett.* **2010**, *104*, 198305.
(35) Hatfield, G. R.; Glans, J. H.; Hammond, W. B. *Macromolecules* **1990**, *23*, 1654.
(36) Adriaensens, P.; Storme, L.; Carleer, R.; D'Hae, J.; Gelan, J.; Litvinov, V. M.; Marissen, R.; Crevecoeur, J. *Macromolecules* **2001**, *35*, 135.
(37) Xu, Z.; Gao, C. *Macromolecules* **2010**, *43*, 6716.
(38) Borggreve, R. J. M.; Gaymans, R. J.; Schuijer, J.; Housz, J. F. I. *Polymer* **1987**, *28*, 1489.
(39) Weeding, T. L.; Veeman, W. S.; Gaur, H. A.; Huysmans, W. G. B. *Macromolecules* **1988**, *21*, 2028.
(40) Minoura, N.; Tsukada, M.; Nagura, M. *Polymer* **1990**, *31*, 265.
(41) Santin, M.; Motta, A.; Freddi, G.; Cannas, M. *J. Biomed. Mater. Res.* **1999**, *46*, 382.
(42) Um, I. C.; Kweon, H.; Park, Y. H.; Hudson, S. *Int. J. Biol. Macromol.* **2001**, *29*, 91.
(43) White, J. L.; Wang, X. W. *Macromolecules* **2002**, *35*, 2633.
(44) Teramoto, H.; Kakazu, A.; Yamauchi, K.; Asakura, T. *Macromolecules* **2007**, *40*, 1562.
(45) Dang, Q.; Lu, S.; Yu, S.; Sun, P.; Yuan, Z. *Biomacromolecules* **2010**, *11*, 1796.
(46) Omenetto, F. G.; Kaplan, D. L. *Science* **2010**, *329*, 528.
(47) Brus, J.; Urbanova, M.; Strachota, A. *Macromolecules* **2008**, *41*, 372.